American Journal of Pathology, Vol. 168, No. 1, January 2006

DOI: 10.2353/ajpath.2006.050090

Vascular Biology, Atherosclerosis and Endothelium Biology

Inducible Nitric Oxide Synthase Mediates Prostaglandin H_2 Synthase Nitration and Suppresses Eicosanoid Production

Ruba S. Deeb,* Hao Shen,* Caryn Gamss,* Tatyana Gavrilova,* Barbara D. Summers,* Rosemary Kraemer,* Gang Hao,† Steven S. Gross,*† Muriel Lainé,* Nobuyo Maeda,‡ David P. Hajjar,* and Rita K. Upmacis*

From the Department of Pathology and Laboratory Medicine, Center of Vascular Biology, and the Department of Pharmacology,† Weill Medical College of Cornell University, New York, New York; and the Department of Pathology and Laboratory Medicine,‡ University of North Carolina, Chapel Hill, North Carolina*

Nitric oxide (NO) modulates the biological levels of arachidonate-derived cell signaling molecules by either enhancing or suppressing the activity of prostaglandin H_2 isoforms (PGHS-1 and PGHS-2). Whether NO activates or suppresses PGHS activity is determined by alternative protein modifications mediated by NO and NO-derived species. Here, we show that inducible NO synthase (iNOS) and PGHS-1 co-localize in atherosclerotic lesions of *ApoE*$^{-/-}$ mouse aortae. Immunoblotting and immunohistochemistry revealed Tyr nitration in PGHS-1 in aortic lesions but markedly less in adjacent nonlesion tissue. PGHS-2 was also found in lesions, but 3-nitrotyrosine incorporation was not detected. 3-Nitrotyrosine formation in proteins is considered a hallmark reaction of peroxynitrite, which can form via NO-superoxide reactions in an inflammatory setting. That iNOS-derived NO is essential for 3-nitrotyrosine modification of PGHS-1 was confirmed by the absence of 3-nitrotyrosine in lesions from *ApoE*$^{-/-}$*iNOS*$^{-/-}$ mice. Mass spectrometric studies specifically identified the active site residue Tyr385 as a 3-nitrotyrosine modification site in purified PGHS-1 exposed to peroxynitrite. PGHS-mediated eicosanoid (PGE_2) synthesis was more than fivefold accelerated in cultured *iNOS*$^{-/-}$ versus *iNOS*-expressing mouse aortic smooth muscle cells, suggesting that iNOS-derived NO markedly suppresses PGHS activity in vascular cells. These results further suggest a regulatory role of iNOS in eicosanoid biosynthesis in human atherosclerotic lesions. ***(Am J Pathol 2006, 168:349–362; DOI: 10.2353/ajpath.2006.050090)***

The enzyme prostaglandin H_2 synthase (PGHS, also known as cyclooxygenase) regulates the production of eicosanoids that modulate physiological processes in the vessel wall, contributing to atherosclerosis and thrombosis. These processes include platelet aggregation, control of vascular tone, and the local inflammatory response. PGHS-1, the constitutive form of PGHS, is the predominant isozyme in platelets and mediates production of platelet thromboxane A_2 (TxA_2), a potent platelet agonist and vasoconstrictor. The beneficial effect of aspirin in reducing cardiovascular events is often attributed to inhibition of PGHS-1-mediated platelet TxA_2.[1,2] Prostacyclin (PGI_2), the major product of vascular endothelium,[3] has opposite effects on platelet function and vascular tone and may inhibit thrombus formation by preventing platelet adhesion.[4] PGHS-2, the inducible form of PGHS, is a proinflammatory mediator that is associated with tumorigenesis and atherosclerosis.[5,6] In some settings PGHS-2 may be the major source of PGI_2 under physiological conditions[7] due to its induction in endothelial cells by hemodynamic shear,[8] but PGHS-1 is also suggested to play an important role.[9] The opposing properties of PGI_2 and TxA_2 suggest that a balance between these compounds in the regulation of interactions

Supported in part by the National Institutes of Health (HL-46403 and HL-07423 to D.P.H., HL-80702 and RR-19355 to S.S.G., HL-42630 to N.M., and a T32 training grant in Cardiovascular Biology to D.P.H.); Pfizer Inc. (Atorvastatin research award to R.S.D.); the Abercrombie Foundation; and Philip Morris USA Inc. and Philip Morris International (to R.K.U.).

Accepted for publication September 19, 2005.

C.G. is currently a medical student at the Albert Einstein College of Medicine of Yeshiva University.

Address reprint requests to Dr. Rita K. Upmacis, Department of Pathology and Center of Vascular Biology, Room A626, Weill Medical College of Cornell University, 1300 York Ave., New York, NY 10021. E-mail: rupmacis@med.cornell.edu.

between platelets and the vessel wall may be disrupted during inflammation and atherosclerosis.[10,11]

Eicosanoid production may be modulated by the interaction of the nitric oxide (NO) and arachidonic acid biosynthetic pathways. This interaction can lead to either stimulation or inhibition of PGHS activity, as well as altered transcription of the *PGHS-2* gene.[12–27] Because several different forms of nitrogen oxides (NO_x) may arise in biological systems, it is conceivable that one form of NO_x may activate PGHS whereas another form may lead to inhibition. Indeed, in our previous studies we demonstrated that peroxynitrite ($ONOO^-$) leads to PGHS-1 activation whereas NO leads to inhibition.[17] We also found that $ONOO^-$ can affect PGHS activity by initiating a signaling cascade that leads to arachidonic acid release and subsequent eicosanoid production.[28] Another interaction of $ONOO^-$ and PGHS leads to PGHS nitration, which is correlated with a loss in activity.[29] In this regard, $ONOO^-$ was found to nitrate-purified PGHS-1 as well as PGHS-1 in smooth muscle cells. Importantly, nitrated PGHS-1 has been detected in human atherosclerotic lesions.[29]

Further evidence that the NO and eicosanoid biosynthetic pathways are linked is supported by recently published *in vivo* studies. Mice missing the gene that encodes the inducible form of NO synthase (iNOS) demonstrated a reduced ability to synthesize eicosanoids globally while synthesis of thromboxane was enhanced.[30] A reduction in eicosanoid biosynthesis in inflammatory lesions was also observed after administration of NOS inhibitors to rats.[31,32] Furthermore, inflamed brain tissue from iNOS knockout mice also contains decreased levels of PGE_2 when compared to wild-type mice.[33] Taken together, these results indicate that iNOS-derived NO, or a NO-derived species, causes decreased biosynthesis of eicosanoids. In contrast, the loss or inhibition of NOS upregulates eicosanoid production.[34–38] For example, coronary arteries from wild-type mice vasodilate in response to acetylcholine by a mechanism involving NO from endothelial NOS (eNOS), but eNOS-deficient mice respond principally by a mechanism involving PGHS.[39] Such observations suggest that the PGHS pathway may compensate to maintain near-normal coronary arterial function in response to chronic loss of eNOS in blood vessels. Either way, given the strong link between NO and eicosanoid pathways, it follows that eicosanoid production in the vessel wall may be affected during disease states in which NO production is perturbed, such as atherosclerosis.[40,41]

The apolipoprotein E-deficient ($ApoE^{-/-}$) mouse has been used successfully as an animal model of atherogenesis.[42] The ApoE amphipathic protein stabilizes and solubilizes lipoprotein particles and thus plays a pivotal role in lipoprotein trafficking. ApoE is a constituent of chylomicrons, very low-density lipoprotein, intermediate-density lipoprotein, and high-density lipoprotein and acts as a ligand for the receptor-mediated clearance of these particles.[43] $ApoE^{-/-}$ mice have plasma cholesterol levels that are four to five times greater than normal and develop atherosclerotic lesions spontaneously, even when fed a low-cholesterol diet.[42] The development of $ApoE^{-/-}$ mice that are also deficient in iNOS ($ApoE^{-/-}iNOS^{-/-}$ mice) has been described.[44–46] $ApoE^{-/-}iNOS^{-/-}$ mice are normotensive and, when fed a normal chow diet, develop atherosclerotic lesions in a manner that is indistinguishable from $ApoE^{-/-}$ mice.[44] For this reason, it was initially thought that iNOS-derived NO does not influence lesion progression. However, when lesion progression is accelerated by feeding $ApoE^{-/-}iNOS^{-/-}$ mice a Western diet, lesions are reduced in size compared to $ApoE^{-/-}$ mice.[45,46] These results indicate that iNOS-derived NO is proatherogenic.

The current study was designed to determine whether PGHS nitration is associated with atherosclerosis in the $ApoE^{-/-}$ mouse model and, if so, whether nitration is dependent on the presence of iNOS. Because $iNOS^{-/-}$ mice in a nonatherosclerotic genetic background display a reduced ability to synthesize eicosanoids,[30] we sought to determine whether the absence of iNOS would promote eicosanoid production in a mouse model of atherosclerosis. For this purpose, we cultured smooth muscle cells from $ApoE^{-/-}$ and $ApoE^{-/-}iNOS^{-/-}$ mice and evaluated eicosanoid production under conditions of iNOS activity and inactivity.

Materials and Methods

Animals

The animal protocol used in these studies was reviewed and approved by the Weill Medical College of Cornell University Care and Use Committee. $ApoE^{-/-}iNOS^{-/-}$ mice were generated as described previously.[44] Mice used in these studies were derived from at least six generations of backcross breeding to C57BL/6J mice.[44] $ApoE^{-/-}iNOS^{-/+}$ heterozygote mice were bred to generate pups that were then genotyped for the iNOS allele by Southern blot analysis. Primers that are complimentary to portions of exon 11, exon 12, and neomycin (neo) were used: AGAGTCCTTCATGAAGCACATGCA (exon 11), TCAGCTTCTCATTCTGCCAGATGT (exon 12), and CAATCCATCTTGTTCAATGGCCGA (neo). The primers were mixed one part neo, two parts exon 11, one part exon 12. Wild-type mice contain both exons 11 and 12 and give rise to a larger band (~500 bp) whereas $iNOS^{-/-}$ mice contain exon 11 and neomycin and give rise to a smaller band (~340 bp). $iNOS^{+/-}$ mice give rise to both bands.

Study Design

$ApoE^{-/-}iNOS^{-/-}$ males and females were designated as the experimental group and $ApoE^{-/-}$ littermates (containing $iNOS^{+/+}$) were designated the control group. $ApoE^{-/-}iNOS^{-/+}$ pups were used as breeding mice. In total, we have used ~100 $ApoE^{-/-}$ mice and ~100 $ApoE^{-/-}iNOS^{-/-}$ mice in these studies. At 21 days, the mice were weaned. The mice were fed a Western diet *ad libitum* comprising 21.2% fat (g/100 g), 0.2% cholesterol, and 0% cholate (Harlan Teklad, Indianapolis, IN). At 6 months, the mice in the control and experimental groups

were sacrificed. The mice were weighed before euthanasia and average weights of the *ApoE*$^{-/-}$ and *ApoE*$^{-/-}$ *iNOS*$^{-/-}$ mice (inclusive of both males and females) were 30.0 ± 0.3 g and 29.2 ± 0.7 g, respectively, and were not significantly different. Aortae were removed surgically from the cardiac origination to the iliac bifurcation and frozen at −80°C. Using a dissecting microscope (SMZ-1B; Nikon, Melville, NY), the aortae were cleared of fat, connective tissues, and adventitia, and dissected into portions representing lesions and surrounding tissue, which were then preserved at −80°C. Lesions and surrounding aortic tissue from these animals were used for Western blot and immunoprecipitation experiments, as described below.

Isolation of Smooth Muscle Cells from ApoE$^{-/-}$ *and ApoE*$^{-/-}$*iNOS*$^{-/-}$ *Mice*

The isolation of vascular smooth muscle cells from murine aortae was performed according to a published method.[47] Briefly, mice were sacrificed by CO_2 asphyxiation and secured on a dissecting board. The thorax and abdomen were rinsed (70% ethanol), the skin was removed, and the thorax was opened to expose the heart and lungs. The aorta was dissected from its origin at the left ventricle to the iliac bifurcation. Using a syringe with a 26-gauge needle to puncture the left ventricle, the aorta was flushed with sterile phosphate-buffered saline (3 ml), surgically removed, and placed in a Petri dish covered with Dulbecco's modified Eagle's medium (DMEM) (50 to 100 μl, containing 0.25 μg/ml filter-sterilized fungizone). Using a dissecting microscope, the aorta was cleared of fat, connective tissues, and adventitia. The aorta was transferred to a new Petri dish, covered with DMEM (50 to 100 μl, containing 10% fetal bovine serum (FBS), 1% glutamine, 1% antibiotic-antimycotic; Invitrogen, Carlsbad, CA), and cut into 1- to 2-mm-square pieces. The pieces of aorta were transferred to a small tissue culture tube containing type II collagenase solution (136 μg in culture medium). The tube was placed with the cap loosely attached in a standard tissue culture incubator (37°C, 5% CO_2) for 4 to 6 hours. The tube was removed from the incubator, gently agitated to resuspend the cells, and DMEM was added (3 ml containing 10% FBS, 1% glutamine, 1% antibiotic-antimycotic). The suspension was transferred to a conical polypropylene tube (15 ml) and centrifuged at 300 × *g* for 5 minutes at room temperature. The medium was aspirated and cells were resuspended in fresh medium (5 ml). The suspension was recentrifuged, the cells were resuspended in medium (0.7 to 1 ml) and transferred to a Primaria dish (BD Biosciences, San Diego, CA). The cells were placed in an incubator and left undisturbed for 5 days.

Cells were confirmed as smooth muscle cells based on fluorescence staining with α-smooth muscle cell actin antibody and for their reactivity and lack of reactivity toward calponin and CD31 (platelet endothelial cell adhesion molecule-1, PECAM-1) antibodies, respectively (see below).[47] Cells were grown to confluence in DMEM supplemented with 10% (v/v) FBS and 1% (v/v) glutamine in either six-well plates or 100-mm dishes (containing ~8.8×10^6 cells/dish). All cells were incubated at 37°C in 5% CO_2 in air. Cells were tested for the presence of mycoplasma (*Mycoplasma* PCR ELISA kit; Roche Applied Science, Indianapolis, IN) with negative results. For experiments with suppressed PGHS-2 expression, cells were rendered quiescent using DMEM supplemented with 2% FBS and 1% glutamine for 2 days.[48] Cells between passages one and five were used in experiments.

Detection of Smooth Muscle Cell α-Actin and Calponin in Smooth Muscle Cells Cultured from ApoE$^{-/-}$ *and ApoE*$^{-/-}$*iNOS*$^{-/-}$ *Mice by Fluorescence Staining*

Cells were plated onto chamber slides (Lab-Tek; Nunc, Naperville, IL). When the cells were 50% confluent, they were washed [phosphate-buffered saline (PBS), three times] and fixed in methanol at −20°C (5 minutes). The cells were washed in PBS (three times), blocked in 5% rabbit serum (R-7136; 500 μl/well for 30 minutes; Sigma Chemical Co., St. Louis, MO) and incubated with primary antibody (monoclonal anti-α-smooth muscle actin, clone 1A4, A-2547, 1:200 dilution; Sigma) in 5% rabbit serum overnight at 4°C. A control for nonspecific interactions was performed by incubating cells with an equivalent concentration of mouse IgG (Sigma). The cells were washed in PBS (three times, 5 minutes each) and incubated with secondary antibody (Alexa Fluor 488 rabbit anti-mouse IgG, A-11078, 1:200 dilution; Molecular Probes, Eugene, OR) in 5% rabbit serum (1 hour at room temperature in the dark). Before the end of the incubation, a blue fluorescent 4′,6-diamidino-2-phenylindole, dihydrochloride, nucleic acid stain (2 μg/ml) was also added (5 minutes). The cells were washed (PBS, three times) and coverslips applied with Vectashield mounting medium (Vector Laboratories, Inc., Burlingame, CA). The cells were examined using an upright fluorescence microscope with appropriate filters (BX51; Olympus, Melville, NY). All cells defined by 4′,6-diamidino-2-phenylindole nuclear staining also contained the selective α-smooth muscle actin and were additionally recognized by an antibody directed against the smooth muscle cell-specific protein calponin (mouse monoclonal calponin antibody, C-2687; Sigma), but not by a rat monoclonal antibody against the endothelial marker CD31 (PECAM-1, SC-18916, Santa Cruz) (data not shown). Notably, a previous study using an identical smooth muscle cell isolation method, conservatively estimated the purity of a resulting smooth muscle cell population at 99%.[47] Cells placed in culture are thought to shift from a contractile to a synthetic phenotype that is also adopted by smooth muscle cells found in the intima during atherosclerosis.[49,50] The cells used in our studies possessed similar levels of α-smooth muscle actin and calponin (which are both

markers of contractile function[51]), indicating that they are in a similar state of differentiation. Cells were maintained at low passages (up to passage 5), although we did not see a significant variation in response to higher passage number (up to passage 12).

Lipopolysaccharide (LPS)/Interferon (IFN)-γ Treatment of Smooth Muscle Cells, PGE_2, and Nitrate/Nitrite Measurements

Smooth muscle cells were preincubated in the presence and absence of LPS (from *Escherichia coli* 026:B6, 10 μg/ml; Sigma) and recombinant mouse IFN-γ (100 U/ml; Calbiochem, La Jolla, CA) for 24 hours to induce *PGHS-2* and *iNOS* gene transcription.[52] Culture medium was replaced with fresh DMEM (with 1% glutamine and 10% or 2% FBS) and the cells incubated for 30 minutes to 1 hour at 37°C. The media was removed, stored at −80°C, and fresh DMEM (with 1% glutamine and 10% or 2% FBS) containing arachidonic acid (20 μmol/L) was added to the cells for 30 minutes to 1 hour at 37°C. The supernatant medium was removed and assayed for PGE_2 formation using an enzyme immunoassay kit (GE Health Care, Piscataway, NJ) and for nitrate/nitrite production using a colorimetric assay kit (Cayman Chemical, Ann Arbor, MI). Total protein in the cell lysate was determined by using either the Lowry or modified Lowry method.[53]

Western Blots of Tissue Homogenates and Smooth Muscle Cells

Lesions and surrounding aortic tissue from *ApoE*$^{-/-}$ and *ApoE*$^{-/-}$*iNOS*$^{-/-}$ mice were homogenized with a Tissue Tearor (Dremel, Racine, WI) in a minimum volume (300 to 500 μl) of lysis buffer (50 mmol/L Tris-HCl, pH 8, 10 mmol/L EDTA, 1% Tween 20, 10 μg/ml aprotinin, 10 μg/ml leupeptin, 1 mmol/L phenylmethyl sulfonyl fluoride) and sonicated. The homogenate was centrifuged (13,000 rpm for 10 minutes at 4°C), and the supernatant was used for protein assay and Western blotting. Smooth muscle cells were washed once with PBS and lysed with a lysis buffer (20 mmol/L Tris-HCl, pH 7.5, 1 mmol/L EDTA, 1 mmol/L EGTA, 150 mmol/L NaCl, 2.5 mmol/L sodium pyrophosphate, 1 mmol/L β-glycerolphosphate, 1 mmol/L sodium orthovanadate, 1 mmol/L phenylmethyl sufonyl fluoride, 1% Triton X-100, and 1 μg/ml leupeptin). The cells were scraped, transferred to Eppendorf tubes, vortexed, and placed on ice (30 minutes). Cell lysates were then sonicated and centrifuged (10,000 × *g* for 10 minutes) for clarification. Cell lysate or tissue protein (15 to 35 μg) was separated by sodium dodecyl sulfate-polyacrylamide gel electrophoresis (10% acrylamide gel), transferred to a nitrocellulose membrane, blocked (90 minutes at 25°C or overnight at 4°C) with 5% nonfat milk in PBS-1% Tween buffer. The membrane was then probed with primary antibody (for PGHS-1, PGHS-2, or iNOS) in 1% nonfat milk in PBS-1% Tween buffer according to the manufacturer's recommendations. When using PGHS-1 antibody (mouse monoclonal, 160110; Cayman Chemical), the membrane was probed for 1 hour, followed by a horseradish peroxidase-conjugated purified goat anti-mouse antibody for 1 hour. When using PGHS-2 antibody (goat polyclonal, SC-1745; Santa Cruz Biotechnology, Santa Cruz, CA), the membrane was probed either 1 hour or overnight, followed by a rabbit anti-goat secondary antibody for 1 hour. When using iNOS antibody (rabbit polyclonal, SC-650; Santa Cruz), the membrane was probed overnight, followed by a goat anti-rabbit secondary antibody for 1 hour. Actin (goat polyclonal, SC-1615, Santa Cruz) or α-smooth muscle actin antibody was used as a measurement of loading accuracy (90 minutes followed by rabbit anti-goat secondary antibody). The immunoblot signal was visualized through chemiluminescence (ECL plus; GE Health Care).

Immunoprecipitation of Nitrated PGHS-1 from Aortic Lesions and Surrounding Tissue in ApoE$^{-/-}$ and ApoE$^{-/-}$iNOS$^{-/-}$ Mice

Lesions and surrounding aortic tissue from *ApoE*$^{-/-}$ and *ApoE*$^{-/-}$*iNOS*$^{-/-}$ mice were homogenized separately and centrifuged as described above for Western blotting. The resulting supernatant (1 mg/ml in PBS) was preclarified with Protein G-agarose beads (25 μl of a 50% slurry in PBS for 30 minutes) to reduce nonspecific binding. The lysate/bead mixture was centrifuged (5000 × *g* for 5 minutes, followed by 16,000 × *g* for 1 minute) to remove the beads, and the clarified lysate was then incubated (overnight at 4°C) with polyclonal nitrotyrosine antibody (Upstate Biotechnology, Lake Placid, NY) followed by Protein G-agarose beads (35 μl of a 50% slurry overnight at 4°C). The bound agarose beads were collected by centrifugation (5000 × *g* for 10 minutes, followed by 16,000 × *g* for 1 minute), washed three times with PBS, and resuspended in Laemmli sample buffer (40 μl). The bead-immunocomplex was boiled (5 minutes), and the sample (40 μl) was separated by sodium dodecyl sulfate-polyacrylamide gel electrophoresis (10%) and immunoblotted with monoclonal PGHS-1 antibody as described above.

Immunohistochemical Localization of PGHS-1 and iNOS

Immunohistochemistry was performed on frozen aortic root sections removed from *ApoE*$^{-/-}$ and *ApoE*$^{-/-}$*iNOS*$^{-/-}$ mice that were maintained on a Western diet for 4 months. Murine hearts were removed and cryopreserved in a 30% sucrose:OCT solution (1:1; Sakura Finetek USA, Inc., Torrance, CA). Serial frozen sections were obtained by cryostat sectioning in the region of the aortic leaflet. The frozen sections were air-dried onto microscopic slides and were treated with H_2O_2 (0.1%) in methanol at −20°C for 30 minutes to quench endogenous peroxidase activity. Adjacent sections were incubated overnight at 4°C with either PGHS-2 (goat polyclonal, SC-1745; Santa Cruz) or iNOS (rabbit polyclonal, SC-650; Santa Cruz) antibodies. Sections were exposed

at room temperature for 1 hour to biotinylated horse anti-goat (BA9500; Vector Laboratories) or biotinylated goat anti-rabbit (BA1000, Vector Laboratories) secondary antibodies, respectively. Immunoreactive proteins were detected using an avidin-biotin-based peroxidase system, using VIP chromogenic substrate (Vector Laboratories). Counterstaining was achieved using hematoxylin. Control sections were treated with PGHS-2 or iNOS antibodies that were previously incubated with blocking peptides (SC-1745P, PGHS-2 blocking peptide; SC-650P iNOS blocking peptide; Santa Cruz) and then developed as described above. Sections were visualized by light microscopy, and digital images were captured using an Olympus microscope.

Double Immunofluorescence of Co-Localized PGHS-2 and iNOS

Sections, prepared as above, were incubated overnight at 4°C with both PGHS-1 (goat polyclonal, SC-1754; Santa Cruz) and nitrotyrosine (rabbit polyclonal, 06284; Upstate Biotechnology) antibodies. The sections were exposed at room temperature for 1 hour to a biotinylated horse anti-goat secondary antibody (BA9500, Vector Laboratories), followed by exposure to rhodamine/avidin (A-2012, Vector Laboratories) for visualization of PGHS-1 and to a fluorescein-labeled goat anti-rabbit secondary antibody (FI-100, Vector Laboratories) for visualization of nitrotyrosine. Control sections were treated with PGHS-1 and nitrotyrosine antibodies that were previously incubated with a PGHS-1 blocking peptide (SC-1754P, Santa Cruz) and 3-nitrotyrosine (10 mmol/L). The fluorescence from immunoreactive proteins was observed by fluorescence microscopy and digital images were captured using an Olympus microscope.

LC-MS/MS Analysis and Database Search

Nanoflow liquid chromatography-tandem mass spectrometry (nLC-MS/MS) was used to identify sites of Tyr nitration in ovine PGHS-1. Ovine PGHS-1 was purified from sheep seminal vesicles as described previously.[54] MS/MS analyses were performed using an 1100 series LC/MSD XCT plus ion trap mass spectrometer (Agilent, Palo Alto, CA). The mobile phase contained 0.1% formic acid in 3% acetonitrile (solvent A) and 0.1% formic acid in 100% acetonitrile (solvent B). PGHS-1 (8 μmol/L in 13 μl, containing heme) was incubated with $ONOO^-$ (1000 μmol/L) for 1 hour at ambient temperature. $ONOO^-$-treated and nontreated control proteins were precipitated in 2 vol of acetone, centrifuged, and then resolubilized in ammonium bicarbonate (20 mmol/L, pH 8). After reduction by dithiothreitol (10 mmol/L, 30 minutes at 50°C) and alkylation by iodoacetamide (50 mmol/L, 30 minutes at ambient temperature), the samples were digested with trypsin (sequencing grade, 1:100, trypsin:PGHS-1; Promega, Madison, WI) for 8 hours at 37°C. Samples were diluted 100-fold with solvent A, and 8 μl of the digested peptide mixture was injected onto a 0.3 × 5 mm Zorbax 300SB-C18 enrichment column at a flow rate of 10 μl/minute. Peptides were subsequently resolved on a 0.075 × 150 mm Zorbax 300SB-C18 analytical column (3.5 μm particle size) at a flow rate of 0.3 μl/min with a gradient of 10 to 40% solvent B for 40 minutes and 40 to 80% solvent B for 30 minutes. Mass spectra were acquired in the automated MS/MS mode, in which MS/MS scans were performed on the three most intense ions after each MS scan. The MS/MS spectra were used to identify the sites of Tyr nitration in PGHS-1 by a database search using SpectrumMill software (Millenium Pharmaceuticals, Cambridge, MA). The parameters for searching were minimum matched peak intensity of 50%, precursor mass tolerance of 2.5 Da, and product mass tolerance of 0.7 Da. The program was instructed to account for Tyr nitration when matching peptide fragments to PGHS-1.

Isolation of Total RNA and Northern Blotting

Aortic smooth muscle cells cultured from *ApoE*$^{-/-}$ and *ApoE*$^{-/-}$*iNOS*$^{-/-}$ mice were lysed in RNA-BEE (Tel-Test, Friendswood, TX). RNA was extracted with chloroform, and then precipitated with isopropanol. Total RNA from each sample was loaded on 1% formaldehyde-agarose gels (20 μg/lane). After electrophoresis, RNA was transferred to a Zeta-probe blotting membrane (Bio-Rad, Hercules, CA). The blot was UV cross-linked and prehybridized with Hybrisol I (Chemicon, Temecula, CA). The blot was then probed using ^{32}P-labeled PGHS-1, followed by rehybridization with ^{32}P-labeled GAPDH (glyceraldehyde-3-phosphate dehydrogenase) to verify that loading in the wells was equal. The PGHS-1 and GAPDH probes were kindly provided by Dr. David L. DeWitt (Michigan State University, East Lansing, MI). The PGHS-2 probe was kindly provided by Dr. Raymond Dubois (Vanderbilt University Medical Center, Nashville, TN).

Statistical Analyses

Data are presented as means ± SE with significant differences determined by *t*-test, with $P < 0.05$ defined as statistically significant.

Results

PGHS-2 is Present in Aortic Lesions in ApoE$^{-/-}$ *and ApoE*$^{-/-}$*iNOS*$^{-/-}$ *Mice but Absent from the Surrounding Tissue*

Figure 1 shows the levels of PGHS-2 and iNOS protein found by Western blot analysis in the plaque (P) and surrounding media (M) in aortae removed surgically from *ApoE*$^{-/-}$ and *ApoE*$^{-/-}$*iNOS*$^{-/-}$ mice after feeding a Western diet for 6 months. Because the tissue samples were small, it was necessary to pool samples from several mice before analysis. Although PGHS-2 and iNOS proteins were both present in the aortic plaque of *ApoE*$^{-/-}$ mice, they were missing or barely detectable in the media surrounding these lesions. In addition, PGHS-2

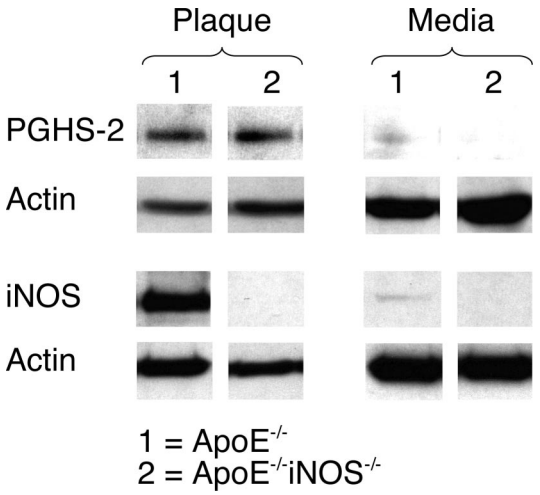

Figure 1. PGHS-2 is present in aortic plaque in *ApoE*$^{-/-}$ and *ApoE*$^{-/-}$ *iNOS*$^{-/-}$ mice but is absent in the surrounding medial tissue. Western blot demonstrating PGHS-2 and iNOS protein levels in atherosclerotic plaque (P) and surrounding media (M) removed from *ApoE*$^{-/-}$ (1) and *ApoE*$^{-/-}$ *iNOS*$^{-/-}$ (2) mice after 6 months on a Western diet. Actin protein levels are also included to demonstrate equal loading of wells. The results shown were obtained by pooling tissue from 11 *ApoE*$^{-/-}$ and 19 *ApoE*$^{-/-}$ *iNOS*$^{-/-}$ mice. The results from this experiment have been reproduced three times from three different pools of tissue.

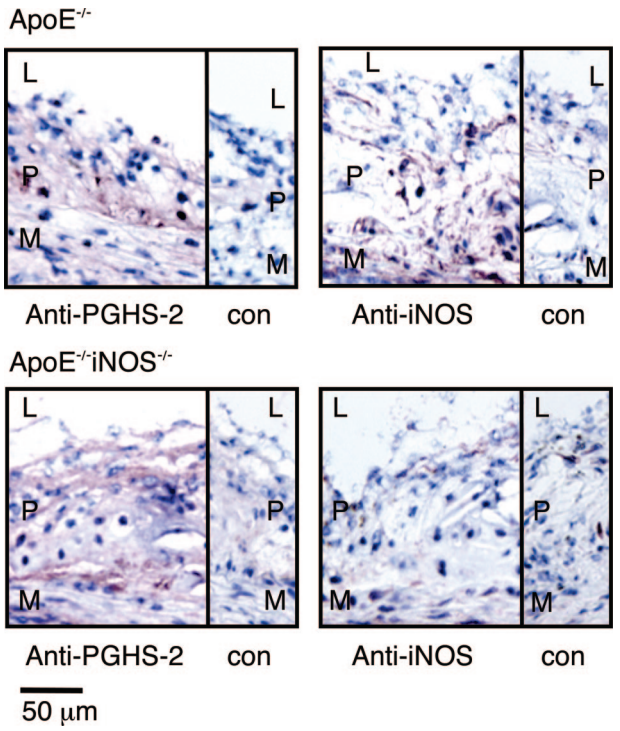

Figure 2. A comparison of PGHS-2 and iNOS localization in aortic sinus lesions from *ApoE*$^{-/-}$ and *ApoE*$^{-/-}$ *iNOS*$^{-/-}$ mice. Immunohistochemical detection of iNOS and PGHS-2 in aortic sinus lesions from *ApoE*$^{-/-}$ (**top**) and *ApoE*$^{-/-}$ *iNOS*$^{-/-}$ (**bottom**) mice fed a Western diet for 4 months. L, lumen; P, plaque; M, media; con, control sections stained with antibody preincubated with antigen. Sections were counterstained with hematoxylin to visualize nuclei. Similar results were observed in aortic sinus lesions from three *ApoE*$^{-/-}$ and three *ApoE*$^{-/-}$ *iNOS*$^{-/-}$ mice.

protein was present in the aortic plaque of *ApoE*$^{-/-}$ *iNOS*$^{-/-}$ mice, but absent from the media. Western blot results confirmed that iNOS protein was missing in both the plaque and the surrounding media of the *ApoE*$^{-/-}$ *iNOS*$^{-/-}$ mice.

To investigate the potential co-localization of PGHS-2 and iNOS in aortic tissue, immunohistochemical analysis was performed on aortic root sections from *ApoE*$^{-/-}$ and *ApoE*$^{-/-}$*iNOS*$^{-/-}$ mice. Immunohistochemical analysis of aortic sinus lesions demonstrated increased PGHS-2 immunoreactivity in the plaque (P) (Figure 2) with little or no expression in the media (M) in both *ApoE*$^{-/-}$ and *ApoE*$^{-/-}$*iNOS*$^{-/-}$ mice. iNOS was detected in lesions from *ApoE*$^{-/-}$ mice, but was missing, as expected, in aortic sections from *ApoE*$^{-/-}$*iNOS*$^{-/-}$ mice. Some iNOS staining was also detected in the medial layer of sections from *ApoE*$^{-/-}$ mice, which is consistent with the observation that by Western blotting some iNOS was present in the tissue that surrounds the lesions in *ApoE*$^{-/-}$ mice (Figure 1). Increased levels of iNOS have previously been localized to vascular smooth muscle cells and mononuclear leukocytes in lesions.[55,56] The expression pattern for both iNOS and PGHS-2 in *ApoE*$^{-/-}$ and *ApoE*$^{-/-}$ *iNOS*$^{-/-}$ lesions was similar to that described by other investigators.[45,46,57]

Lesions from ApoE$^{-/-}$ *Mice Contain Nitrated PGHS-1 that Is Absent in ApoE*$^{-/-}$*iNOS*$^{-/-}$ *Mice*

Immunoprecipitation experiments were performed to determine whether nitrated PGHS accumulates in aortic tissue obtained from *ApoE*$^{-/-}$ and *ApoE*$^{-/-}$*iNOS*$^{-/-}$ mice. Animals were maintained on a Western diet for 6 months, and aortic tissue was dissected under a microscope into portions comprising the plaque (P) and surrounding media (M). Because the tissue samples were small, it was necessary to pool samples from several mice for ample immunoprecipitation of PGHS-1. Antioxidants were added to limit potential *ex vivo* oxidation. Lesions were readily visualized and were commonly ~1 mm in length but sometimes reached 3 to 4 mm. For every immunoprecipitation experiment, tissues were pooled from ~10 *ApoE*$^{-/-}$ and ~10 *ApoE*$^{-/-}$*iNOS*$^{-/-}$ mice, providing ~300 μg of total protein. Nitrated proteins from the atherosclerotic plaque and surrounding media were immunoprecipitated using a polyclonal 3-nitrotyrosine antibody. Immunoprecipitated proteins were resolved by gel electrophoresis and immunoblotted with a PGHS-1 monoclonal antibody (Figure 3). Although nitrated PGHS-1 was observed in the plaque from *ApoE*$^{-/-}$ mice, little or no PGHS-1 nitration was detected in plaque obtained from the *ApoE*$^{-/-}$*iNOS*$^{-/-}$ animals. In addition, the surrounding media showed little or no evidence of PGHS-1 nitration in either the *ApoE*$^{-/-}$ or *ApoE*$^{-/-}$ *iNOS*$^{-/-}$ mice. These data indicate that lesional PGHS-1 undergoes significant Tyr nitration *in vivo* and iNOS is the principal source of NO required for this modification. Surprisingly, on stripping of blots and reprobing for PGHS-2, we did not observe PGHS-2 nitration (data not shown).

To confirm that PGHS-1 is nitrated *in situ*, double-label immunofluorescence imaging was performed on sections

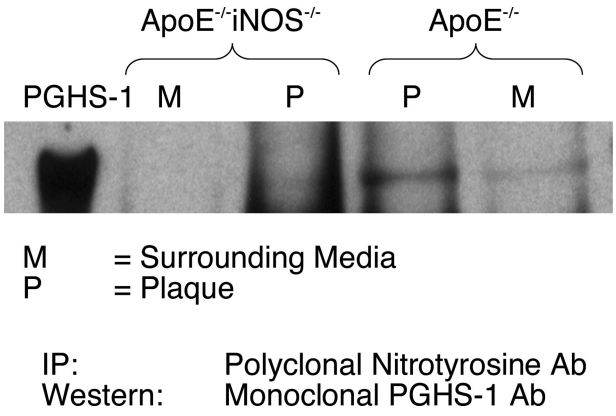

Figure 3. Lesions from *ApoE*$^{-/-}$ mice contain nitrated PGHS-1 that is reduced in *ApoE*$^{-/-}$*iNOS*$^{-/-}$ mice. Aortic tissue from *ApoE*$^{-/-}$ and *ApoE*$^{-/-}$*iNOS*$^{-/-}$ mice fed a Western diet for 6 months was dissected into portions representing the plaques (P) and noninvolved surrounding medial tissue (M). The tissue was homogenized as described in the Materials and Methods. Proteins containing 3-nitrotyrosine were immunoprecipitated using a polyclonal 3-nitrotyrosine antibody and then immunoblotted with a PGHS-1 monoclonal antibody. This experiment has been reproduced three times using three different pools of tissue. Each tissue pool is from ~10 *ApoE*$^{-/-}$ and ~10 *ApoE*$^{-/-}$*iNOS*$^{-/-}$ mice.

of murine hearts from *ApoE*$^{-/-}$ and *ApoE*$^{-/-}$*iNOS*$^{-/-}$ mice fed a Western diet for 4 months. Double immunofluorescence detected PGHS-1 (Figure 4a) and nitrotyrosine (Figure 4b) in lesions of the *ApoE*$^{-/-}$ mouse. The overlay demonstrated co-localization of PGHS-1 and nitrotyrosine in lesions of the *ApoE*$^{-/-}$ mouse (yellow; indicated by arrows in Figure 4c). In contrast, in lesions of *ApoE*$^{-/-}$*iNOS*$^{-/-}$ mice, PGHS-1 was present in the plaque (Figure 4d), but nitrotyrosine levels were low (Figure 4e). Moreover, co-localization of PGHS-1 and nitrotyrosine in *ApoE*$^{-/-}$*iNOS*$^{-/-}$ mice was reduced (Figure 4f). These data indicate that nitrated PGHS-1 predominates in the plaque of lesions obtained from *ApoE*$^{-/-}$ mice relative to *ApoE*$^{-/-}$*iNOS*$^{-/-}$ mice, although the presence of some nitrated PGHS-1 in aortic lesions of *ApoE*$^{-/-}$*iNOS*$^{-/-}$ mice cannot be discounted.

Reaction of PGHS-1 with Peroxynitrite Results in 3-Nitrotyrosine Accumulation at Tyr385

We previously demonstrated that purified PGHS-1 can be nitrated by $ONOO^-$.[29] Spectroscopic data indicated that $ONOO^-$ nitrates ~2 Tyr residues/PGHS-1 monomer.[29,58] To identify which Tyr residues were nitrated, $ONOO^-$-treated purified PGHS-1 was subjected to trypsinolysis and analyzed by nLC-MS/MS. PGHS-1 was incubated with $ONOO^-$ (1 mmol/L) for 1 hour and isolated by acetone precipitation. PGHS-1 was resuspended in ammonium bicarbonate, reduced, and alkylated (see Materials and Methods). Solubilized PGHS-1 was proteolyzed with 0.3% trypsin, followed by peptide analysis using nLC-MS/MS (Figure 5). Figure 5a shows the extracted ion chromatograms for the $ONOO^-$-treated PGHS-1 and control PGHS-1 samples of a fragment corresponding to m/z (645.6) of the quadruply charged peptide ion IAMEFNQLYHWHPLMPDSFR (Ile377 to Arg396), which is nitrated on Tyr385. Notably, this nitrated peptide from $ONOO^-$-treated PGHS-1 (~38 minutes, indicated by an arrow) was undetectable in nontreated, control PGHS-1. Tandem mass spectrometric analysis of this peptide (Figure 5b) confirms that this peak indeed represents the tryptic peptide containing nitrated Tyr385. Several y- and b-series ions are observed, including a long, continuous series of y ions that stretches from y12 to y19 of this peptide fragment. It is notable that the fragmentation pattern of peptides is sequence-dependent, and many peptides do not display an ideal fragmentation pattern with a more complete b- and y-ion series. This is particularly relevant for a peptide such as IAMEFNQLYHWHPLMPDSFR, which contains two Pro and two His residues. It is well known that both of these residues induce atypical fragmentation.[59] With two His and Pro each in the sequence, it is, therefore, not surprising that the fragmentation pattern observed for this peptide is somewhat limited. Figure 5b shows that the MS/MS spectrum is dominated by a triply charged y18 ion at m/z = 798.9, in accord with the presence of two positively charged His residues in the sequence. The identity of this ion is further supported by another strong peak at m/z = 599.4 representing the quadruply charged ion of the same fragment. The strong dominancy of this particular fragment may account for the relatively less complete ion series detected. In a previously published tandem mass spectrometric study of a variant form of the human hemoglobin α chain, a very similar fragmentation pattern of a quadruply charged tryptic peptide ion bearing two His residues was observed: the MS/MS was dominated by a few triply charged y ions near the N terminus, with incomplete b- and y-ion series.[60] Site-directed mutagenesis studies have demonstrated that Tyr385 is essential to cyclooxygenase activity.[61,62] Technical limitations have precluded the rigorous MS/MS-based structural characterization of PGHS-1 from lesional tissues, owing mainly to the very limited amount of available tissue. These data establish that $ONOO^-$ selectively nitrates Tyr385 in PGHS-1, but it is not yet known whether this specific Tyr residue is nitrated in PGHS-1 in atherosclerotic tissue, and if so, whether this is the preferred Tyr residue that undergoes nitration under biological conditions.

Smooth Muscle Cells Cultured from ApoE$^{-/-}$*iNOS*$^{-/-}$ *Mice Express Significantly Higher Levels of PGHS-1 and PGHS-2 Protein and mRNA than Smooth Muscle Cells from ApoE*$^{-/-}$ *Mice*

Smooth muscle cells were cultured from *ApoE*$^{-/-}$ and *ApoE*$^{-/-}$*iNOS*$^{-/-}$ mice to examine the levels of PGHS-1 and PGHS-2 expressed. Cells were maintained in FBS, which has previously been shown to induce PGHS-2 in rat smooth muscle cells.[48,63] To determine the effect of serum on PGHS-2 expression, smooth muscle cells were grown in media containing 10% FBS, which was then replaced with 2% FBS. Figure 6 demonstrates that PGHS-2 was expressed when smooth muscle cells from *ApoE*$^{-/-}$ mice were incubated in media containing 10%

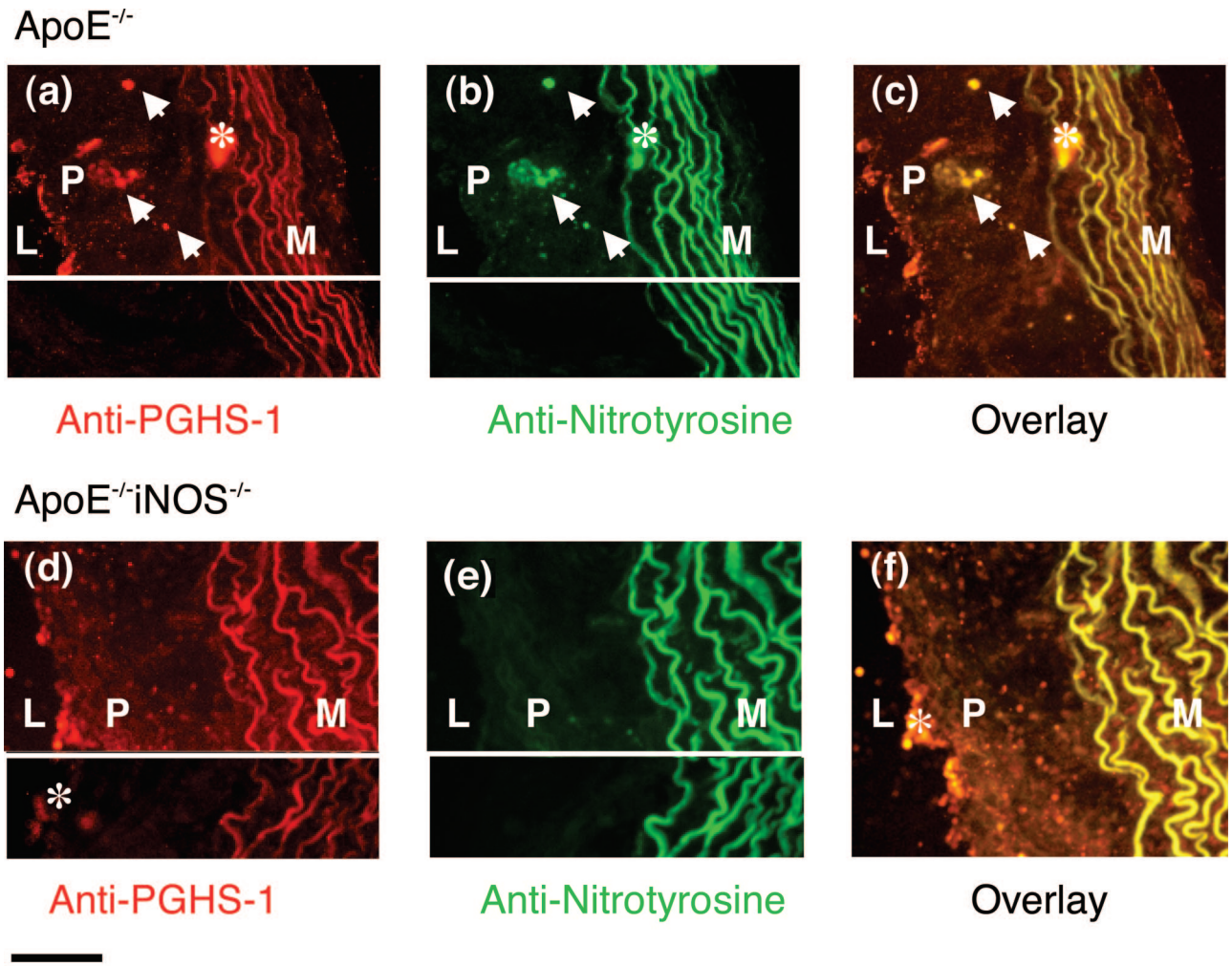

Figure 4. PGHS-1 and nitrotyrosine co-localize in aortic sinus lesions from *ApoE*$^{-/-}$ mice. Double-immunofluorescence detection of PGHS-1 and nitrotyrosine in aortic sinus lesions removed from *ApoE*$^{-/-}$ (**a–c**) and *ApoE*$^{-/-}$*iNOS*$^{-/-}$ (**d–f**) mice maintained on a Western diet for 4 months. For visualization of PGHS-1, sections were incubated with a goat polyclonal PGHS-1 antibody followed by exposure to a biotinylated horse anti-goat secondary antibody and a rhodamine/avidin mixture. Sections were co-incubated with a fluorescein-labeled goat anti-rabbit secondary antibody for visualization of nitrotyrosine. The **left** sides of these panels depict autofluorescence from the internal elastic lamina in the media. **Asterisks** denote areas of nonspecific binding or autofluorescence. **Insets** (**bottom parts** of **a**, **b**, **d**, and **e**) represent control sections in which the PGHS-1 and nitrotyrosine antibodies were pretreated with a PGHS-1 blocking peptide and 3-nitrotyrosine (10 mmol/L), respectively. PGHS-1 and nitrotyrosine co-localization was assessed in aortic sinus sections from three *ApoE*$^{-/-}$ and three *ApoE*$^{-/-}$*iNOS*$^{-/-}$ mice.

FBS (day 0). However, PGHS-2 levels progressively diminished with time when replaced by 2% FBS (days 1 to 4). Thus, smooth muscle cells cultured in FBS express PGHS-2.

Western blot analyses were performed on smooth muscle cells from *ApoE*$^{-/-}$ and *ApoE*$^{-/-}$*iNOS*$^{-/-}$ mice cultured under identical conditions to determine the relative expression of PGHS-1 and PGHS-2 protein levels. Figure 7 shows that significantly higher levels of both PGHS-1 (Figure 7a) and PGHS-2 (Figure 7b) protein were found in aortic smooth muscle cells obtained from adult *ApoE*$^{-/-}$*iNOS*$^{-/-}$ mice compared to *ApoE*$^{-/-}$ mice. Under these conditions, iNOS protein was missing in the *ApoE*$^{-/-}$*iNOS*$^{-/-}$ smooth muscle cells, but traces were occasionally detected by Western blotting in the *ApoE*$^{-/-}$ cells (data not shown). Under quiescent conditions (ie, in DMEM containing 2% FBS), PGHS-1 protein levels were also significantly higher in smooth muscle cells from *ApoE*$^{-/-}$*iNOS*$^{-/-}$ mice compared to *ApoE*$^{-/-}$, although no differences were observed in the low levels of PGHS-2 (data not shown). Figure 7 also shows that significantly higher levels of PGHS-1 (Figure 7c) and PGHS-2 (Figure 7d) mRNA levels were expressed in cells obtained from *ApoE*$^{-/-}$*iNOS*$^{-/-}$ mice compared to *ApoE*$^{-/-}$ control mice (when normalized to GAPDH mRNA levels).

Smooth Muscle Cells Cultured from ApoE$^{-/-}$ *and ApoE*$^{-/-}$*iNOS*$^{-/-}$ *Mice Produce Significantly Different Levels of Eicosanoids*

Smooth muscle cells cultured from *ApoE*$^{-/-}$ and *ApoE*$^{-/-}$*iNOS*$^{-/-}$ mice were exposed to arachidonic acid (20 μmol/L) and the supernatant medium was analyzed for

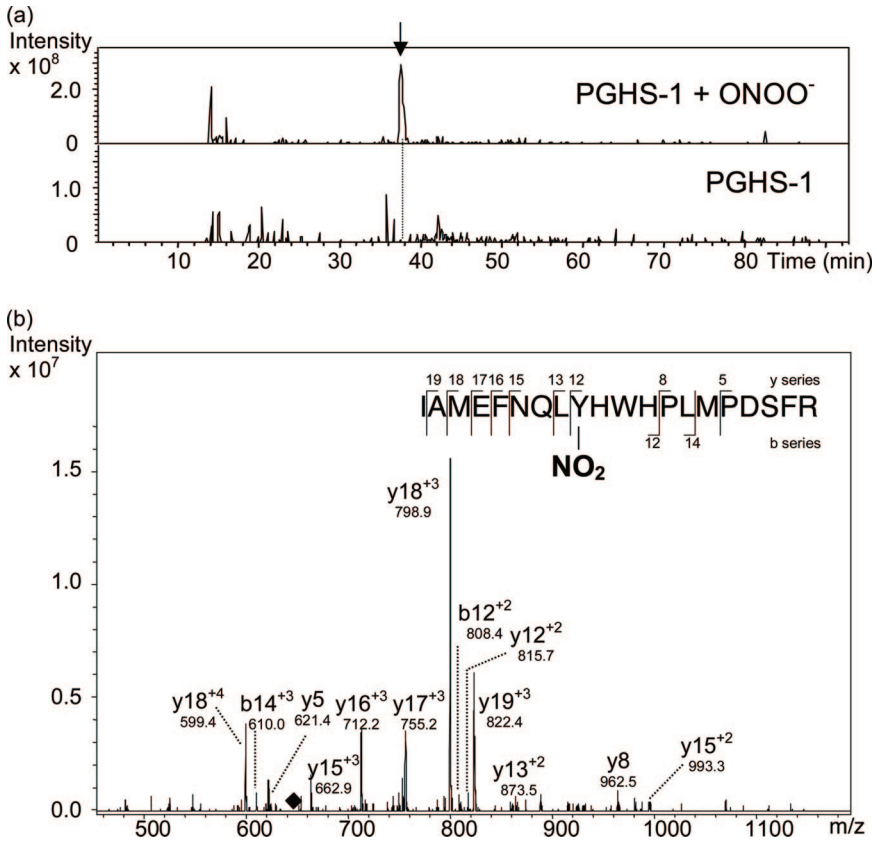

Figure 5. Peroxynitrite nitrates purified PGHS-1 at Tyr385. Purified ovine PGHS-1 (8 μmol/L) was incubated with peroxynitrite ($ONOO^-$; 1 mmol/L) for 1 hour and subjected to acetone precipitation, resuspension in ammonium bicarbonate, and reduction and alkylation (as described in Materials and Methods). A control PGHS-1 sample was prepared in a similar manner. The samples were digested with 0.3% trypsin overnight and analyzed by nLC-MS/MS. **a:** Extracted ion chromatograms for the peptide fragment (m/z = 645.6) representing the quadruply charged peptide IAMEFNQLYHWHPLMPDSFR that is nitrated at the Tyr residue. The **top** and **bottom** extracted ion chromatograms monitor this peptide fragment with time for the $ONOO^-$-treated and control PGHS-1 samples, respectively. The **arrow** at ~38 minutes in the **top** profile indicates the presence of a peak that is missing in the control PGHS-1 sample. **b:** MS/MS analysis of the peptide fragment at ~38 minutes confirms the identity of this peptide sequence as IAMEFNQLYHWHPLMPDSFR containing nitrated Tyr385. The **black diamond** at m/z = 645.6 indicates the position of the precursor fragment from which the ions observed are derived.

PGE_2 formation. Figure 8 shows that in the absence of added arachidonic acid, basal levels of PGE_2 produced by cultured *ApoE*$^{-/-}$ and *ApoE*$^{-/-}$*iNOS*$^{-/-}$ smooth muscle cells were low. On addition of arachidonic acid (20 μmol/L), increased levels of PGE_2 were produced in both cases compared to basal levels. However, *ApoE*$^{-/-}$*iNOS*$^{-/-}$ smooth muscle cells produced significantly higher levels of PGE_2 compared to *ApoE*$^{-/-}$ smooth muscle cells. After incubation with IFN-γ and LPS, which are known to synergistically induce both PGHS-2 and iNOS expression,[52] significantly higher levels of PGE_2 were once again observed in the supernatant medium from *ApoE*$^{-/-}$*iNOS*$^{-/-}$ compared to *ApoE*$^{-/-}$ smooth muscle cells after arachidonic acid addition (20 μmol/L). When challenged with LPS/IFN-γ, *ApoE*$^{-/-}$ and *ApoE*$^{-/-}$*iNOS*$^{-/-}$ smooth muscle cells produced similar levels of PGHS-2 with no significant differences (data not shown). Nitrite/nitrate production and iNOS expression under these conditions, however, was observed in *ApoE*$^{-/-}$ mice but not in *ApoE*$^{-/-}$*iNOS*$^{-/-}$ mice (data not shown). Interestingly, there was no significant difference between PGE_2 produced by arachidonic acid-stimulated *ApoE*$^{-/-}$*iNOS*$^{-/-}$ cells in the presence or absence of LPS/IFN-γ, suggesting that the *ApoE*$^{-/-}$*iNOS*$^{-/-}$ cells produce maximal levels of PGHS-2.

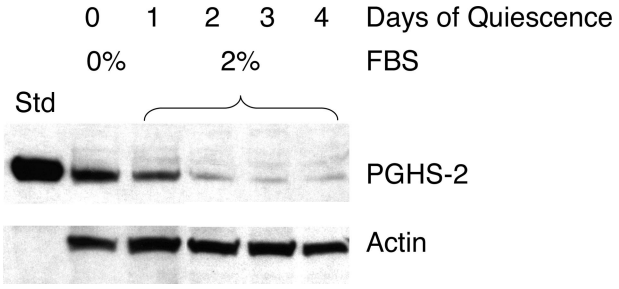

Figure 6. Serum induces PGHS-2 in smooth muscle cells. Aortic smooth muscle cells were cultured from *ApoE*$^{-/-}$ mice as described in Materials and Methods. The cells were grown to ~80% confluency in DMEM containing 10% FBS (**lane 0**) and in DMEM containing 2% FBS for 1, 2, 3, or 4 days (**lanes 1–4**, respectively). The cells were lysed, analyzed by Western blotting, and probed for PGHS-2, followed by actin. Std represents standard purified ovine PGHS-2.

These data indicate that significantly higher PGE_2 levels were produced by smooth muscle cells cultured from *ApoE*$^{-/-}$*iNOS*$^{-/-}$ than *ApoE*$^{-/-}$ mice. This result is consistent with the observation that *ApoE*$^{-/-}$*iNOS*$^{-/-}$ cells express more PGHS-1 and PGHS-2 mRNA and protein than *ApoE*$^{-/-}$ cells. In addition, smooth muscle cells cultured from *ApoE*$^{-/-}$*iNOS*$^{-/-}$ mice were maximally stimulated with respect to PGHS-2 expression and were

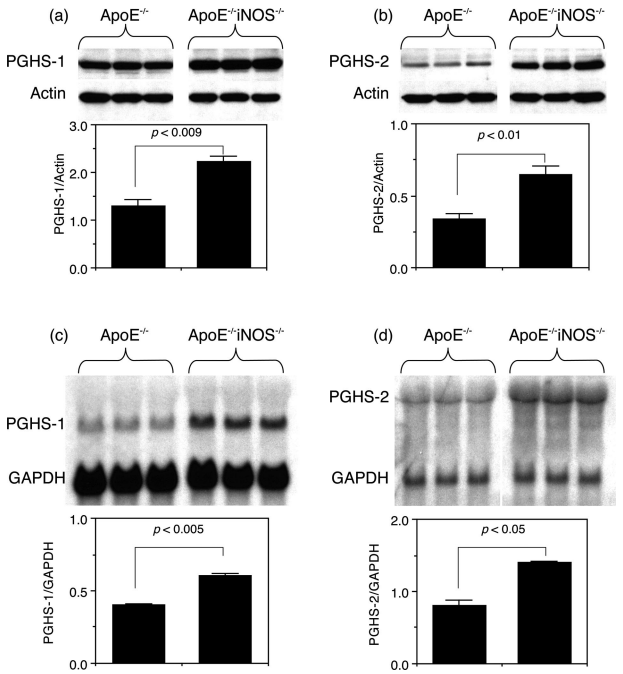

Figure 7. PGHS-1 and PGHS-2 protein and mRNA levels are significantly higher in smooth muscle cells cultured from $ApoE^{-/-}iNOS^{-/-}$ than $ApoE^{-/-}$ mice. Aortic smooth muscle cells were cultured from $ApoE^{-/-}$ and $ApoE^{-/-}iNOS^{-/-}$ mice as described in Materials and Methods. The cells were grown to confluency in DMEM containing 10% FBS, then lysed and analyzed in triplicate for PGHS-1 (**a**) and PGHS-2 (**b**) protein by Western blotting. In each case, the blot was also probed for actin. The bar graphs represent the protein/actin ratio for **a** and **b**. The results are representative of one experiment (with three replicates) that was repeated three times. RNA was also isolated from $ApoE^{-/-}$ and $ApoE^{-/-}iNOS^{-/-}$ smooth muscle cells that were cultured in DMEM containing 10% FBS. **c:** After isolation, RNA (20 μg per lane) was loaded onto a gel in triplicate and separated by electrophoresis, transferred to a nylon membrane, and hybridized with a ^{32}P-labeled probe for PGHS-1 to yield a signal at 2.8 kb. The blot was then rehybridized with a ^{32}P-labeled GAPDH cDNA probe (signal at 1.3 kb). **d:** The same blot was later rehybridized with a ^{32}P-labeled cDNA probe for PGHS-2 to yield a signal at 4.3 kb. The bar graphs represent the PGHS-1/GAPDH (**c**) and PGHS-2/GAPDH (**d**) ratios. The results are representative of one experiment repeated twice.

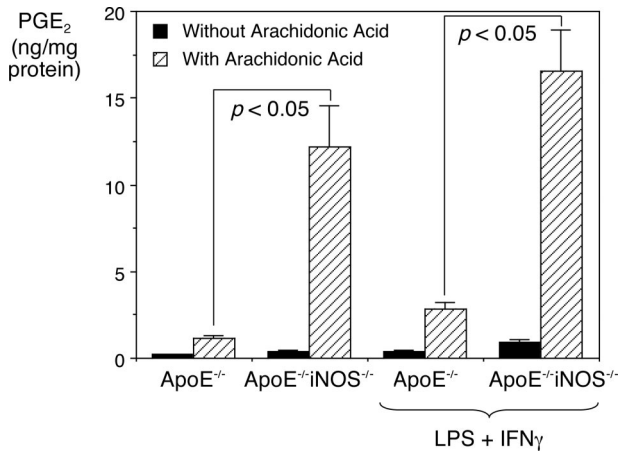

Figure 8. PGE_2 production is significantly higher in $ApoE^{-/-}iNOS^{-/-}$ than in $ApoE^{-/-}$ smooth muscle cells. Aortic smooth muscle cells were cultured from $ApoE^{-/-}$ and $ApoE^{-/-}iNOS^{-/-}$ mice as described in Materials and Methods. The cells were grown in DMEM containing 10% FBS to 90% confluency, and then incubated in DMEM with and without LPS (10 μg/ml) and IFN-γ (100 U/ml) at 37°C. After 24 hours, the supernatant was replaced with fresh DMEM containing 10% FBS and the cells incubated at 37°C. After 1 hour, the medium was removed and stored at −80°C. The cells were then exposed to DMEM (10% FBS) containing arachidonic acid (20 μmol/L) and incubated at 37°C. After 1 hour, the supernatant was removed and stored at −80°C. The supernatants were analyzed for PGE_2 formation. The data represent the average from three experiments in which three measurements were recorded per experiment.

not influenced by the addition of LPS/IFN-γ. Although LPS/IFN-γ challenge in $ApoE^{-/-}$ smooth muscle cells produced a modest increase in PGE_2 over basal levels, the levels produced did not match those achieved by the $ApoE^{-/-}iNOS^{-/-}$ cells. These results further suggest a regulatory role of iNOS on PGHS activity.

Discussion

This study demonstrates for the first time that iNOS influences PGHS expression and activity and contributes to PGHS-1 nitration during the disease state of atherosclerosis. Owing to the numbers of mice required for this study, both male and female $ApoE^{-/-}$ and $ApoE^{-/-}iNOS^{-/-}$ mice were used and no attempt was made to determine the effects of gender.

PGHS-2 and iNOS have previously been observed in human atherosclerotic tissue,[5,6,64–66] and levels of PGHS-2 were also found to be increased in murine atherosclerotic aortae.[57,67] In this current study, we demonstrate that PGHS-2 is present in the murine atherosclerotic lesions of $ApoE^{-/-}$ and $ApoE^{-/-}iNOS^{-/-}$ mice fed a Western diet for 6 months but is absent in the tissue surrounding the lesion. In addition, we show that iNOS is induced in lesions in $ApoE^{-/-}$ mice and is virtually absent in the surrounding tissue. As expected, iNOS is absent in both lesions and surrounding noninvolved tissues obtained from the $ApoE^{-/-}iNOS^{-/-}$ mice.

We have previously observed PGHS-1 nitration in human atherosclerotic tissue obtained from endarterectomies.[29] We now report that PGHS-1 is nitrated in lesions obtained from $ApoE^{-/-}$ mice but markedly less so in lesions from $ApoE^{-/-}iNOS^{-/-}$ mice. Notably, immunofluorescence data does not exclude the possibility that PGHS-1 nitration may occur at low levels in the absence of iNOS. Accordingly, eNOS may contribute to PGHS-1 nitration, although PGHS-1 nitration is primarily dependent on iNOS protein expression. The coincidental lack of PGHS-1 nitration and iNOS in the surrounding noninvolved aortic tissue in the $ApoE^{-/-}$ mouse seems to suggest, however, that PGHS-1 nitration is iNOS-dependent.

Our data demonstrate that iNOS is involved in PGHS-1 nitration at the site of the atherosclerotic lesion and that iNOS provides the first step in a mechanism of PGHS-1 nitration. NO release from iNOS could combine with superoxide to form peroxynitrite ($ONOO^-$), a reactive species with enhanced oxidizing capability.[68,69] Of the deleterious effects, $ONOO^-$ has been implicated in myocardial reoxygenation injury,[70] initiating lipid peroxidation of membranes,[71] reacting with sulfhydryl groups of proteins,[72] and causing oxidative damage by introducing Tyr nitration.[73] We have previously demonstrated that $ONOO^-$ causes nitration of purified PGHS-1 and PGHS-1 in smooth muscle cells.[29] In this study, we now identify Tyr385 as a specific site of nitration by $ONOO^-$ in purified PGHS-1 by mass spectrometry. Tyr385 is located at the

apex of the cyclooxygenase binding channel and is thought to be involved in the catalytic mechanism of PGHS enzymes.[61,62] Tyr385 is involved in radical formation that initiates arachidonic acid oxygenation, leading to eicosanoid formation,[74,75] although the radical may also be localized on a different Tyr residue.[62,76–79] Nitration of Tyr385 would predictably lead to a complete loss of arachidonic acid metabolism.[61] Although NO has previously been demonstrated to couple with the Tyr385 radical of PGHS-1,[80] leading to the eventual nitration of Tyr385,[81] this represents the first identification of a specific nitrated Tyr residue in PGHS-1 by $ONOO^-$.

Under pathophysiological conditions, $ONOO^-$ formation may occur, because both iNOS expression and superoxide production are concomitantly elevated,[64,65,82] and the rate of $ONOO^-$ production (6.7×10^9 mol/$L^{-1}second^{-1}$) outcompetes the rate at which superoxide dismutase scavenges superoxide (2×10^9 mol/$L^{-1}second^{-1}$).[68,83] Thus, the presence of $ONOO^-$ during atherosclerosis seems likely, although doubts over its formation under physiological or pathophysiological conditions persist.[84–86] Other mechanisms can also lead to nitrotyrosine formation. For instance, peroxidase enzymes (eg, myeloperoxidase, MPO) can use nitrite (NO_2^-) and hydrogen peroxide (H_2O_2) as substrates to catalyze tyrosine nitration in proteins.[87–89] The MPO/NO_2^-/H_2O_2 system has been demonstrated to nitrate and to cause LDL oxidation, which may contribute to the development of atherosclerosis.[90] On the other hand, others have shown that *MPO*$^{-/-}$ mice show greater levels of nitrotyrosine formation (and larger infarct volumes) than wild-type mice, leading to the conclusion that the presence of MPO counters nitration.[91] In the absence of a peroxidase, NO_2^- and H_2O_2 can nitrate at low pH (<2).[92] Nitrotyrosine formation in proteins may also occur in the presence of hypochlorous acid (HOCl) and NO_2^-, but this reaction also yields 3-chlorotyrosine,[93,94] which may also cause oxidative damage in tissues.[95] Despite these alternative mechanisms, nitration of Tyr residues in proteins produces a stable end-product that can be detected immunologically. Identification of nitrated PGHS-1 in lesions from *ApoE*$^{-/-}$ mice by mass spectrometry has not yet proven feasible (due to the large amounts of tissue required coupled with the necessity of having reasonably pure samples), but it is the subject of ongoing efforts. Further studies will be required to elucidate the mechanism by which Tyr nitration in PGHS-1 occurs in atherosclerotic tissue and whether Tyr385 in PGHS-1 represents a physiological target for nitration.

We have previously demonstrated that PGHS nitration coincides with a loss in activity,[29] but it is unclear whether the extent of nitration and associated loss in function contributes to the progression of atherosclerosis. Surprisingly, PGHS-2 nitration was not detected, suggesting that this modification does not occur to a significant extent or possibly that antibodies used are not sufficiently sensitive for detection. Although it is generally assumed that PGHS-2 is the most important isozyme in atherosclerosis and inflammation, PGHS-1 may also play a key role in maintaining the balance of eicosanoids during this disease state.[67]

Previous studies have found that endothelial NO synthase (eNOS) is an important regulator of vascular function. Thus, *ApoE*$^{-/-}$*eNOS*$^{-/-}$ mice were found to have higher blood pressure and increased atherosclerotic lesion size compared to normotensive, atherosclerotic *ApoE*$^{-/-}$ mice.[44] The lack of eNOS in *ApoE*$^{-/-}$ mice caused them to develop kidney damage and have decreased kidney weight with glomerular lipid deposition and calcification.[44] The inducible form of NOS is usually absent in nondiseased vessels, and thus may not be expected to contribute to vascular function under normal conditions. However, under conditions of inflammation, iNOS is induced and is capable of generating NO, possibly in the μm range.[96] A genetic lack of *iNOS* in *ApoE*$^{-/-}$ mice does not affect blood pressure nor alter the development of atherosclerotic lesions as compared to *ApoE*$^{-/-}$ mice when fed a normal chow diet.[44] However, when *ApoE*$^{-/-}$*iNOS*$^{-/-}$ mice are fed a high-fat diet, the atherosclerotic lesions are diminished in size compared to *ApoE*$^{-/-}$ mice.[45,46] Our experience from performing immunoprecipitation experiments indicated that lesions from ~5 *ApoE*$^{-/-}$ and ~9 *ApoE*$^{-/-}$*iNOS*$^{-/-}$ mice (at 6 months on a high cholesterol diet) typically provided enough protein for one such experiment. The difference in the numbers of mice required likely reflects the fact that less lesion formation occurs in *ApoE*$^{-/-}$*iNOS*$^{-/-}$ mice than in *ApoE*$^{-/-}$ mice fed a Western diet[46] and indicates that iNOS contributes to lesion size under these dietary conditions (possibly via protein nitration). Cholesterol, cholesteryl esters, and lipoperoxides (a marker for oxidative stress) have been found to be significantly diminished in *ApoE*$^{-/-}$*iNOS*$^{-/-}$ mice compared to *ApoE*$^{-/-}$ mice.[45,46] These results indicate that iNOS contributes to the size of atherosclerotic lesions in *ApoE*$^{-/-}$ mice, perhaps by promoting inflammation and oxidative stress at the site of the lesion.

Finally, we show that smooth muscle cells cultured from *ApoE*$^{-/-}$*iNOS*$^{-/-}$ mice express significantly higher levels of PGHS-1 and PGHS-2, as well as increased levels of PGE_2, compared to those cultured from *ApoE*$^{-/-}$ mice. Cells challenged with LPS and IFN-γ, immunoactivators known to induce iNOS as well as PGHS-2, did not boost PGE_2 levels in *ApoE*$^{-/-}$ cells to the high levels obtained from *ApoE*$^{-/-}$*iNOS*$^{-/-}$ cells. Northern blot analysis of PGHS-1 and PGHS-2 mRNA demonstrated that both *PGHS-1* and *PGHS-2* transcription are elevated in *ApoE*$^{-/-}$*iNOS*$^{-/-}$ compared to *ApoE*$^{-/-}$ smooth muscle cells. The effect of iNOS deletion on eicosanoid production has previously been studied in mice.[30] It was found that PGE_2 production was decreased in peritoneal macrophages and in urine obtained from *iNOS*$^{-/-}$ mice compared to wild-type mice. These observations are consistent with NO or NO-derived species having a stimulatory effect on PGHS in inflammatory cells and in the kidney. Indeed, $ONOO^-$ is known to stimulate purified PGHS and PGHS in cells[16,17] and could explain why higher levels of urinary and macrophage eicosanoids are observed in wild-type mice. Our current study investigated the effect of iNOS deletion in a mouse model of atherosclerosis (ie, using *ApoE*$^{-/-}$ mice). Previous investigations have demonstrated that urinary eicosanoid levels are elevated in

human and murine atherosclerosis (using either *ApoE*$^{-/-}$ or low-density lipoprotein receptor knockout, *LDLR*$^{-/-}$, mice).[9–11] Although the measurement of urinary eicosanoids represents a noninvasive method, the levels are not specific to the tissue of origin of these compounds. We chose, therefore, to investigate levels of eicosanoids produced by smooth muscle cells cultured from both *ApoE*$^{-/-}$ and *ApoE*$^{-/-}$*iNOS*$^{-/-}$ mice. Surprisingly, we have observed that iNOS deletion in *ApoE*$^{-/-}$ mice has a stimulatory effect on PGHS-1 and PGHS-2 pretranslational levels. Others have demonstrated that in the absence of eNOS, other vasodilator pathways compensate to maintain near-normal coronary arterial function.[39] In this regard, coronary arteries from wild-type mice responded to acetylcholine by a mechanism involving NO from eNOS; however, coronary arteries from *eNOS*$^{-/-}$ mice dilated by a mechanism dependent on PGHS. These observations suggest a compensatory ability by PGHS in response to chronic loss of NOS, which has also been reported by others.[34–38] It is conceivable that mechanisms may exist that compensate for the lack of iNOS. Because PGHS-mediated PGE_2 production is increased in cultured *ApoE*$^{-/-}$*iNOS*$^{-/-}$ versus *ApoE*$^{-/-}$ (iNOS-expressing) mouse aortic smooth muscle cells, we infer that iNOS can markedly suppress PGHS activity in vascular cells. The extent to which iNOS-dependent nitration of Tyr in PGHS-1 contributes to perturbed eicosanoid biosynthesis in human atherosclerotic lesions awaits future investigations.

Acknowledgments

We thank Drs. Qi Ling and Arun Deora for their help in establishing the breeding and genotyping of mice; Catherine Beale for occasional maintenance of mouse colonies; Barbara Ferris for the technical help provided with culturing and staining of smooth muscle cells; Dr. Hideaki Nakaya (Keio University, Tokyo, Japan) for technical help provided with Northern blotting; Leona Cohen-Gould and Mekalia Sutherland in the Electron Microscopy and Histology Core Facility of Weill Medical College for the preparation of aortic root cryosections; and Dr. Andrew Nicholson for helpful suggestions.

References

1. Ridker PM, Cushman M, Stampfer MJ, Tracy RP, Hennekens CH: Inflammation, aspirin, and the risk of cardiovascular disease in apparently healthy men. N Engl J Med 1997, 336:973–979
2. Wu K: Aspirin and other cyclooxygenase inhibitors: new therapeutic insights. Semin Vasc Med 2003, 3:107–112
3. Moncada S, Gryglewski R, Bunting S, Vane JR: An enzyme isolated from arteries transforms prostaglandin endoperoxides to an unstable substance that inhibits platelet aggregation. Nature 1976, 263:663–665
4. Moncada S: Prostacyclin and arterial wall biology. Arteriosclerosis 1982, 2:193–207
5. Baker CS, Hall RJ, Evans TJ, Pomerance A, Maclouf J, Creminon C, Yacoub MH, Polak JM: Cyclooxygenase-2 is widely expressed in atherosclerotic lesions affecting native and transplanted human coronary arteries and colocalizes with inducible nitric oxide synthase and nitrotyrosine particularly in macrophages. Arterioscler Thromb Vasc Biol 1999, 19:646–655
6. Schonbeck U, Sukhova GK, Graber P, Coulter S, Libby P: Augmented expression of cyclooxygenase-2 in human atherosclerotic lesions. Am J Pathol 1999, 155:1281–1291
7. McAdam BF, Catella-Lawson F, Mardini IA, Kapoor S, Lawson JA, FitzGerald GA: Systemic biosynthesis of prostacyclin by cyclooxygenase (COX)-2: the human pharmacology of a selective inhibitor of COX-2. Proc Natl Acad Sci USA 1999, 96:272–277
8. Topper JN, Cai J, Falb D, Gimbrone MA: Identification of vascular endothelial genes differentially responsive to fluid mechanical stimuli: cyclooxygenase-2, manganese superoxide dismutase, and endothelial cell nitric oxide synthase are selectively up-regulated by steady laminar shear stress. Proc Natl Acad Sci USA 1996, 93:10417–10422
9. Belton O, Byrne D, Kearney D, Leahy A, Fitzgerald DJ: Cyclooxygenase-1 and -2-dependent prostacyclin formation in patients with atherosclerosis. Circulation 2000, 102:840–845
10. FitzGerald GA, Smith B, Pedersen AK, Brash AR: Increased prostacyclin biosynthesis in patients with severe atherosclerosis and platelet activation. N Engl J Med 1984, 310:1065–1068
11. Pratico D, Cyrus T, Li H, FitzGerald GA: Endogenous biosynthesis of thromboxane and prostacyclin in 2 distinct murine models of atherosclerosis. Blood 2000, 96:3823–3826
12. Salvemini D, Misko TP, Masferrer JL, Seibert K, Currie MG, Needleman P: Nitric oxide activates cyclooxygenase enzymes. Proc Natl Acad Sci USA 1993, 90:7240–7244
13. Salvemini D, Seibert K, Masferrer JL, Misko TP, Currie MG, Needleman P: Endogenous nitric oxide enhances prostaglandin production in a model of renal inflammation. J Clin Invest 1994, 93:1940–1947
14. Hajjar DP, Lander HM, Pearce SF, Upmacis RK, Pomerantz KB: Nitric oxide enhances prostaglandin-H synthase-1 activity by a heme-independent mechanism: evidence implicating nitrosothiols. J Am Chem Soc 1995, 117:3340–3346
15. Maccarrone M, Putti S, Finazzi Agro A: Nitric oxide donors activate the cyclo-oxygenase and peroxidase activities of prostaglandin H synthase. FEBS Lett 1997, 410:470–476
16. Landino LM, Crews BC, Timmons MD, Morrow JD, Marnett LJ: Peroxynitrite, the coupling product of nitric oxide and superoxide, activates prostaglandin biosynthesis. Proc Natl Acad Sci USA 1996, 93:15069–15074
17. Upmacis RK, Deeb RS, Hajjar DP: Regulation of prostaglandin H_2 synthase activity by nitrogen oxides. Biochemistry 1999, 38:12505–12513
18. Kanner J, Harel S, Granit R: Nitric oxide, an inhibitor of lipid oxidation by lipoxygenase, cyclooxygenase and hemoglobin. Lipids 1992, 27:46–49
19. Tsai AL, Wei C, Kulmacz RJ: Interaction between nitric oxide and prostaglandin H synthase. Arch Biochem Biophys 1994, 313:367–372
20. Curtis JF, Reddy NG, Mason RP, Kalyanaraman B, Eling TE: Nitric oxide: a prostaglandin H synthase 1 and 2 reducing cosubstrate that does not stimulate cyclooxygenase activity or prostaglandin H synthase expression in murine macrophages. Arch Biochem Biophys 1996, 335:369–376
21. Davidge ST, Baker PN, Laughlin MK, Roberts JM: Nitric oxide produced by endothelial cells increases production of eicosanoids through activation of prostaglandin H synthase. Circ Res 1995, 77:274–283
22. Corbett JA, Kwon G, Turk J, McDaniel ML: IL-1 beta induces the coexpression of both nitric oxide synthase and cyclooxygenase by islets of Langerhans: activation of cyclooxygenase by nitric oxide. Biochemistry 1993, 32:13767–13770
23. Tetsuka T, Daphna-Iken D, Srivastava SK, Baier LD, Du Maine J, Morrison AR: Cross-talk between cyclooxygenase and nitric oxide pathways: prostaglandin E_2 negatively modulates induction of nitric oxide synthase by interleukin 1. Proc Natl Acad Sci USA 1994, 91:12168–12172
24. Inoue T, Fukuo K, Morimoto S, Koh E, Ogihara T: Nitric oxide mediates interleukin-1-induced prostaglandin E2 production by vascular smooth muscle cells. Biochem Biophys Res Commun 1993, 194:420–424
25. Mollace V, Colasanti M, Rodino P, Lauro GM, Rotiroti D, Nistico G: NMDA-dependent prostaglandin E2 release by human cultured astroglial cells is driven by nitric oxide. Biochem Biophys Res Commun 1995, 215:793–799

26. Molina-Holgado F, Lledo A, Guaza C: Evidence for cyclooxygenase activation by nitric oxide in astrocytes. Glia 1995, 15:167–172
27. Tetsuka T, Daphna-Iken D, Miller BW, Guan Z, Baier LD, Morrison AR: Nitric oxide amplifies interleukin 1-induced cyclooxygenase-2 expression in rat mesangial cells. J Clin Invest 1996, 97:2051–2056
28. Upmacis RK, Deeb RS, Resnick MJ, Lindenbaum R, Gamss C, Mittar D, Hajjar DP: Involvement of the mitogen-activated protein kinase cascade in peroxynitrite-mediated arachidonic acid release in vascular smooth muscle cells. Am J Physiol 2004, 286:C1271–C1280
29. Deeb RS, Resnick MJ, Mittar D, McCaffrey T, Hajjar DP, Upmacis RK: Tyrosine nitration in prostaglandin H_2 synthase. J Lipid Res 2002, 43:1718–1726
30. Marnett LJ, Wright TL, Crews BC, Tannenbaum SR, Morrow JD: Regulation of prostaglandin biosynthesis by nitric oxide is revealed by targeted deletion of inducible nitric-oxide synthase. J Biol Chem 2000, 275:13427–13430
31. Sautebin L, Ialenti A, Ianaro A, Di Rosa M: Modulation by nitric oxide of prostaglandin biosynthesis in the rat. Br J Pharmacol 1995, 114:323–328
32. Salvemini D, Settle SL, Masferrer JL, Seibert K, Currie MG, Needleman P: Regulation of prostaglandin production by nitric oxide; an in vivo analysis. Br J Pharmacol 1995, 114:1171–1178
33. Nogawa S, Forster C, Zhang F, Nagayama M, Ross ME, Iadecola C: Interaction between inducible nitric oxide synthase and cyclooxygenase-2 after cerebral ischemia. Proc Natl Acad Sci USA 1998, 95:10966–10971
34. Puybasset L, Bea ML, Ghaleb B, Giudicelli JF, Berdeaux A: Coronary and systemic hemodynamic effects of sustained inhibition of nitric oxide synthesis in conscious dogs. Evidence for cross talk between nitric oxide and cyclooxygenase in coronary vessels. Circ Res 1996, 79:343–357
35. Henrion D, Dechaux E, Dowell FJ, Maclour J, Samuel JL, Levy BI, Michel JB: Alteration of flow-induced dilatation in mesenteric resistance arteries of L-NAME treated rats and its partial association with induction of cyclo-oxygenase-2. Br J Pharmacol 1997, 121:83–90
36. Beverelli F, Bea ML, Puybasset L, Giudicelli JF, Berdeaux A: Chronic inhibition of NO synthase enhances the production of prostacyclin in coronary arteries through upregulation of the cyclooxygenase type 1 isoform. Fundam Clin Pharmacol 1997, 11:252–259
37. Sun D, Huang A, Smith CJ, Stackpole CJ, Connetta JA, Shesely EG, Koller A, Kaley G: Enhanced release of prostaglandins contributes to flow-induced arteriolar dilation in eNOS knockout mice. Circ Res 1999, 85:288–293
38. Osanai T, Fujita N, Fujiwara N, Nakano T, Takahashi K, Guan W, Okumura K: Cross talk of shear-induced production of prostacyclin and nitric oxide in endothelial cells. Am J Physiol 2000, 278:H233–H238
39. Lamping KG, Nuno DW, Shesely EG, Maeda N, Faraci FM: Vasodilator mechanisms in the coronary circulation of endothelial nitric oxide synthase-deficient mice. Am J Physiol 2000, 279:H1906–H1912
40. Loscalzo J, Welch G: Nitric oxide and its role in the cardiovascular system. Prog Cardiovasc Dis 1995, 38:87–104
41. Cox DA, Vita JA, Treasure CB, Fish RD, Alexander RW, Ganz P, Selwyn AP: Atherosclerosis impairs flow-mediated dilation of coronary arteries in humans. Circulation 1989, 80:458–465
42. Zhang SH, Reddick RL, Piedrahita JA, Maeda N: Spontaneous hypercholesterolemia and arterial lesions in mice lacking apolipoprotein E. Science 1992, 258:468–471
43. Mahley RW: Apolipoprotein E: cholesterol transport protein with expanding role in cell biology. Science 1988, 240:622–630
44. Knowles JW, Reddick RL, Jennette JC, Shesely EG, Smithies O, Maeda N: Enhanced atherosclerosis and kidney dysfunction in $eNOS^{-/-}ApoE^{-/-}$ mice are ameliorated by enalapril treatment. J Clin Invest 2000, 105:451–458
45. Detmers PA, Hernandez M, Mudgett J, Hassing H, Burton C, Mundt S, Chun S, Fletcher D, Card DJ, Lisnock J, Weikel R, Bergstrom JD, Shevell DE, Hermanowski-Vosatka A, Sparrow CP, Chao YS, Rader DJ, Wright SD, Pure E: Deficiency in inducible nitric oxide synthase results in reduced atherosclerosis in apolipoprotein E-deficient mice. J Immunol 2000, 165:3430–3435
46. Kuhlencordt PJ, Chen J, Han F, Astern J, Huang PL: Genetic deficiency of inducible nitric oxide synthase reduces atherosclerosis and lowers plasma lipid peroxides in apolipoprotein E-knockout mice. Circulation 2001, 103:3099–3104
47. Ray JL, Leach R, Herbert JM, Benson M: Isolation of vascular smooth muscle cells from a single murine aorta. Methods Cell Sci 2001, 23:185–188
48. Rimarachin JA, Jacobson JA, Szabo P, Maclouf J, Creminon C, Weksler BB: Regulation of cyclooxygenase-2 expression in aortic smooth muscle cells. Arterioscler Thromb 1994, 14:1021–1031
49. Thyberg J: Differentiated properties and proliferation of arterial smooth muscle cells in culture. Int Rev Cytol 1996, 169:183–265
50. Thyberg J: Phenotypic modulation of smooth muscle cells during formation of neointimal thickenings following vascular injury. Histol Histopathol 1998, 13:871–891
51. Shanahan C, Weissberg P: Smooth muscle cell heterogeneity: patterns of gene expression in vascular smooth muscle cells in vitro and in vivo. Arterioscler Thromb Vasc Biol 1998, 18:333–338
52. Pomerantz KB, Hajjar DP, Levi R, Gross SS: Cholesterol enrichment of arterial smooth muscle cells upregulates cytokine-induced nitric oxide synthesis. Biochem Biophys Res Commun 1993, 191:103–109
53. Markwell MA, Haas SM, Bieber LL, Tolbert NE: A modification of the Lowry procedure to simplify protein determination in membrane and lipoprotein samples. Anal Biochem 1978, 87:206–210
54. Malkowski MG, Theisen MJ, Scharmen A, Garavito RM: The formation of stable fatty acid substrate complexes in prostaglandin H(2) synthase-1. Arch Biochem Biophys 2000, 380:39–45
55. Esaki T, Hayashi T, Muto E, Yamada K, Kuzuya M, Iguchi A: Expression of inducible nitric oxide synthase in T lymphocytes and macrophages of cholesterol-fed rabbits. Atherosclerosis 1997, 128:39–46
56. Behr D, Rupin A, Fabiani JN, Verbeuren TJ: Distribution and prevalence of inducible nitric oxide synthase in atherosclerotic vessels of long-term cholesterol-fed rabbits. Atherosclerosis 1999, 142:335–344
57. Belton O, Duffy A, Toomey S, Fitzgerald D: Cyclooxygenase isoforms and platelet vessel wall interactions in the apolipoprotein E knockout mouse model of atherosclerosis. Circulation 2003, 108:3017–3023
58. Boulos C, Jiang H, Balazy M: Diffusion of peroxynitrite into the human platelet inhibits cyclooxygenase via nitration of tyrosine residues. J Pharm Exp Ther 2000, 293:222–229
59. Paizs B, Suhai S: Fragmentation pathways of protonated peptides. Mass Spectrom Rev 2005, 24:508–548
60. Promé D, Promé J-C: Hb Neuilly-sur-Marne, a new human hemoglobin variant with Ser-Asp-Leu inserted between a86(F7) Leu and a87(F8) His: characterization by high-energy collision-induced dissociation liquid secondary ion mass spectrometry and low energy collision-induced dissociation tandem mass spectrometry in an ion trap fitted with a nanospray ionization source. Eur J Mass Spectrom 2000, 6:205–211
61. Shimokawa T, Kulmacz RJ, De Witt DL, Smith WL: Tyrosine 385 of prostaglandin endoperoxide synthase is required for cyclooxygenase catalysis. J Biol Chem 1990, 265:20073–20076
62. Hsi LC, Hoganson CW, Babcock GT, Garavito RM, Smith WL: An examination of the source of the tyrosyl radical in ovine prostaglandin endoperoxide synthase-1. Biochem Biophys Res Commun 1995, 207:652–660
63. Bailey JM, Muza B, Hla T, Salata K: Restoration of prostacyclin synthase in vascular smooth muscle cells after aspirin treatment: regulation by epidermal growth factor. J Lipid Res 1985, 26:54–61
64. Buttery LD, Springall DR, Chester AH, Evans TJ, Standfield EN, Parums DV, Yacoub MH, Polak JM: Inducible nitric oxide synthase is present within human atherosclerotic lesions and promotes the formation and activity of peroxynitrite. Lab Invest 1996, 75:77–85
65. Wilcox JN, Subramanian RR, Sundell CL, Tracey WR, Pollock JS, Harrison DG, Marsden PA: Expression of multiple isoforms of nitric oxide synthase in normal and atherosclerotic vessels. Arterioscler Thromb Vasc Biol 1997, 17:2479–2488
66. Luoma JS, Stralin P, Marklund SL, Hiltunen TP, Sarkioja T, Yla-Herttuala S: Expression of extracellular SOD and iNOS in macrophages and smooth muscle cells in human and rabbit atherosclerotic lesions: colocalization with epitopes characteristic of oxidized LDL and peroxynitrite-modified proteins. Arterioscler Thromb Vasc Biol 1998, 18:157–167
67. Pratico D, Tillmann C, Zhang ZB, Li H, FitzGerald GA: Acceleration of atherogenesis by COX-1-dependent prostanoid formation in low density lipoprotein receptor knockout mice. Proc Natl Acad Sci USA 2001, 98:3358–3363
68. Huie RE, Padmaja S: The reaction of NO with superoxide. Free Radic Res Commun 1993, 18:195–199

69. Beckman JS, Beckman TW, Chen J, Marshall PA, Freeman BA: Apparent hydroxyl radical production by peroxynitrite: implications for endothelial injury from nitric oxide and superoxide. Proc Natl Acad Sci USA 1990, 87:1620–1624
70. Matheis G, Sherman MP, Buckberg GD, Haybron DM, Young HH, Ignarro LJ: Role of L-arginine-nitric oxide pathway in myocardial reoxygenation injury. Am J Physiol 1992, 262:H616–H620
71. Radi R, Beckman JS, Bush KM, Freeman BA: Peroxynitrite-induced membrane lipid peroxidation: the cytotoxic potential of superoxide and nitric oxide. Arch Biochem Biophys 1991, 288:481–487
72. Radi R, Beckman JS, Bush KM, Freeman BA: Peroxynitrite oxidation of sulfhydryls. The cytotoxic potential of superoxide and nitric oxide. J Biol Chem 1991, 266:4244–4250
73. Ischiropoulos H, al-Mehdi AB: Peroxynitrite-mediated oxidative protein modifications. FEBS Lett 1995, 364:279–282
74. Dietz R, Nastainczyk W, Ruf HH: Higher oxidation states of prostaglandin H synthase. Rapid electronic spectroscopy detected two spectral intermediates during the peroxidase reaction with prostaglandin G_2. Eur J Biochem 1988, 171:321–328
75. Tsai AL, Palmer G, Kulmacz RJ: Prostaglandin H synthase. Kinetics of tyrosyl radical formation and of cyclooxygenase catalysis. J Biol Chem 1992, 267:17753–17759
76. Tsai A, Hsi LC, Kulmacz RJ, Palmer G, Smith WL: Characterization of the tyrosyl radicals in ovine prostaglandin H synthase-1 by isotope replacement and site-directed mutagenesis. J Biol Chem 1994, 269:5085–5091
77. Shi W, Hoganson CW, Espe M, Bender CJ, Babcock GT, Palmer G, Kulmacz RJ, Tsai A: Electron paramagnetic resonance and electron nuclear double resonance spectroscopic identification and characterization of the tyrosyl radicals in prostaglandin H synthase 1. Biochemistry 2000, 39:4112–4121
78. Smith WL, Song I: The enzymology of prostaglandin endoperoxide H synthases-1 and -2. Prostaglandins Other Lipid Mediat 2002, 69:115–128
79. Rogge C, Liu W, Wu G, Wang L, Kulmacz R, Tsai A: Identification of Tyr504 as an alternative tyrosyl radical site in human prostaglandin H synthase-2. Biochemistry 2004, 43:1560–1568
80. Gunther MR, Hsi LC, Curtis JF, Gierse JK, Marnett LJ, Eling TE, Mason RP: Nitric oxide trapping of the tyrosyl radical of prostaglandin H synthase-2 leads to tyrosine iminoxyl radical and nitrotyrosine formation. J Biol Chem 1997, 272:17086–17090
81. Goodwin DC, Gunther MR, Hsi LC, Crews BC, Eling TE, Mason RP, Marnett LJ: Nitric oxide trapping of tyrosyl radicals generated during prostaglandin endoperoxide synthase turnover. Detection of the radical derivative of tyrosine 385. J Biol Chem 1998, 273:8903–8909
82. Ohara Y, Peterson TE, Harrison DG: Hypercholesterolemia increases endothelial superoxide anion production. J Clin Invest 1993, 91:2546–2551
83. Beckman JS, Crow JP: Pathological implications of nitric oxide, superoxide and peroxynitrite formation. Biochem Soc Trans 1993, 21:330–334
84. Pfeiffer S, Mayer B: Lack of tyrosine nitration by peroxynitrite generated at physiological pH. J Biol Chem 1998, 273:27280–27285
85. Pfeiffer S, Lass A, Schmidt K, Mayer B: Protein tyrosine nitration in cytokine-activated murine macrophages. Involvement of a peroxidase/nitrite pathway rather than peroxynitrite. J Biol Chem 2001, 276:34051–34058
86. Pfeiffer S, Lass A, Schmidt K, Mayer B: Protein tyrosine nitration in mouse peritoneal macrophages activated in vitro and in vivo: evidence against an essential role of peroxynitrite. FASEB J 2001, 15:2355–2364
87. van der Vliet A, Eiserich JP, Halliwell B, Cross CE: Formation of reactive nitrogen species during peroxidase-catalyzed oxidation of nitrite. A potential additional mechanism of nitric oxide-dependent toxicity. J Biol Chem 1997, 272:7617–7625
88. Sampson JB, Ye Y, Rosen H, Beckman JS: Myeloperoxidase and horseradish peroxidase catalyze tyrosine nitration in proteins from nitrite and hydrogen peroxide. Arch Biochem Biophys 1998, 356:207–213
89. Eiserich JP, Hristova M, Cross CE, Jones AD, Freeman BA, Halliwell B, van der Vliet A: Formation of nitric oxide-derived inflammatory oxidants by myeloperoxidase in neutrophils. Nature 1998, 391:393–397
90. Leeuwenburgh C, Hardy MM, Hazen SL, Wagner P, Oh-ishi S, Steinbrecher UP, Heinecke JW: Reactive nitrogen intermediates promote low density lipoprotein oxidation in human atherosclerotic intima. J Biol Chem 1997, 272:1433–1436
91. Takizawa S, Aratani Y, Fukuyama N, Maeda N, Hirabayashi H, Koyama H, Shinohara Y, Nakazawa H: Deficiency of myeloperoxidase increases infarct volume and nitrotyrosine formation in mouse brain. J Cereb Blood Flow Metab 2002, 22:50–54
92. Oury TD, Tatro L, Ghio AJ, Piantadosi CA: Nitration of tyrosine by hydrogen peroxide and nitrite. Free Radic Res 1995, 23:537–547
93. Eiserich JP, Cross CE, Jones AD, Halliwell B, van der Vliet A: Formation of nitrating and chlorinating species by reaction of nitrite with hypochlorous acid. A novel mechanism for nitric oxide-mediated protein modification. J Biol Chem 1996, 271:19199–19208
94. Domigan NM, Charlton TS, Duncan MW, Winterbourn CC, Kettle AJ: Chlorination of tyrosyl residues in peptides by myeloperoxidase and human neutrophils. J Biol Chem 1995, 270:16542–16548
95. Hazen SL, Crowley JR, Mueller DM, Heinecke JW: Mass spectrometric quantification of 3-chlorotyrosine in human tissues with attomole sensitivity: a sensitive and specific marker for myeloperoxidase-catalyzed chlorination at sites of inflammation. Free Radic Biol Med 1997, 23:909–916
96. Lefer AM, Scalia R: Nitric oxide in inflammation. Methods Physiol Series 2001, 3:447–472